Adv. Geosci., 63, 1–13, 2023
https://doi.org/10.5194/adgeo-63-1-2023

Advances in Geosciences
Open Access
EGU

Physicochemical Characterization and Origin of Aeolian Sand Dunes in Southeastern Qatar: A Comparative Study with Mediterranean Sand Dunes

Hezam Al-Awah and Wael S. Matter

Geology Program, Department of Chemistry and Earth Sciences, College of Arts and Sciences,
Qatar University, P.O. Box 2713, Doha, Qatar

Correspondence: Wael S. Matter (wmatter@qu.edu.qa)

Received: 10 July 2023 – Revised: 19 September 2023 – Accepted: 20 September 2023 – Published: 12 October 2023

Abstract. A significant geographical feature in Qatar is represented by aeolian sand dunes, which cover approximately 12 % of the country's total surface area and are well-developed in the southern region. This study aims to enhance our understanding of Qatari sand dunes by investigating their textural parameters, chemical composition, mineralogy, potential sources of sediment, and transportation mechanisms. To assess the physical and chemical characteristics of the sand dunes being examined, various experimental techniques were employed, including grain size analyses, X-ray fluorescence, X-ray diffraction, scanning electron microscopy, and energy dispersive spectrometry. The analysis of the studied sand dunes indicates a combination of calcareous and siliceous materials. These dunes predominantly consist of quartz, protoenststite, calcite, and feldspar minerals, with clay minerals being relatively scarce. The chemical composition of the sand samples shows high levels of silicon oxide, significant concentrations of calcium, magnesium, and aluminum oxides, along with smaller amounts of iron, chlorine, potassium, and sulfur oxides. Furthermore, trace elements such as titanium, strontium, chromium, and scandium oxides were found in negligible quantities. Based on the physical and chemical properties observed in the studied sand dunes, it can be inferred that they originate from the Mesopotamian plain, Zagros Mountains, and the calcareous coast of the Arabian Gulf are likely of aeolian origin. The findings derived from our examination of Qatari sand dunes have been compared with published data from the Arabian deserts situated along the Mediterranean Sea. The primary objective of this comparative analysis is to highlight both the common features and distinctive variations in their composition and origins. This comparative assessment suggests that Qatari sand dunes exhibit lower maturity levels in terms of silicon content and may have an origin distinct from those in the Mediterranean region.

1 Introduction

Qatar is located on the eastern portion of the stable shelf of the Arabian Plate. The country's landmass is formed by a major regional NNE-SSW anticline known as the Qatar-South Fars Arch (Rao et al., 2001), which is bounded by the fold-thrust Zagros Belt towards the north (Powers et al., 1966; Boukhary, 1985; Alsharhan and Nairn, 1995; Al-Saad and Ibrahim, 2002). The surface of Qatar is mostly characterized by low to moderate relief, with the highest elevations measuring 103 m above sea level located in the southern western part of the peninsula (Scheibert et al., 2005).

The surface area of Qatar is mainly covered by Lower Eocene to Pleistocene limestones and dolostones, interbedded with marls, shales, clays, and gypsum (Al-Yousef, 2003; Al-Saad, 2005). The country also has exposures of Upper Miocene to Pliocene clastics (continental gravel and sandy conglomerate), as well as aeolian sand dunes, sand sheets, sabkha, and beach deposits of Pleistocene to Holocene age. The supratidal to intertidal sabkha and beach deposits are located along the coastal zone.

Aeolian sand dunes are the most significant topographic feature in Qatar, covering approximately 12 % of the country's total surface area. They are primarily formed by the action of the long-term regional NW Shamal wind and are well-developed in the southern part of the country (Michel et al.,

2018; Engel et al., 2018). Isolated barchan dunes are the most common type of aeolian sand dunes in Qatar, although other types such as compound barchans, longitudinal and transverse dunes also occur (Ashour, 1985; Embabi and Ashour, 1993). A number of studies have been published on Qatari sand dunes, including research on the physical, chemical and spectral characteristics of these dunes (Ashour, 1985; Embabi and Ashour, 1993; Sadiq and Howari, 2009; Al-Ansary et al., 2012; Sankaran et al., 2022).

The Arabian deserts along the Mediterranean region display a notable geological phenomenon in the shape of sand dunes. These dunes are a product of intricate interactions among geological, meteorological, and climatic factors, which significantly influence their physicochemical characteristics.The objective of this study is to provide a better understanding of Qatari sand dunes by examining their textural parameters, chemical composition, mineralogy, possible sediment source, and mode of transportation.

The findings arising from the study of Qatari sand dunes will be juxtaposed with comparable data from the Arabian deserts adjacent to the Mediterranean Sea. The primary objective of this comparison is to underscore both the commonalities and distinctions in their composition and origin.

2 Materials and Methods

2.1 Material Description

For this study, a total of thirty-five sand samples were collected from two locations (A and B) during two field trips (Fig. 1). The samples were collected from five different sand dunes in the southern region of Qatar, with sampling conducted across different parts of the dunes, including the tails, middle, and crest of both the windward and leeward sides. Area A yielded sixteen samples, consisting of eight from a long dune (AL) and eight from a short dune (AS). Meanwhile, area B provided nineteen samples, with eight from a long dune (BL), eight from a short dune (BS), and three from a dune located directly along the coast (BC) (Table 1). All collected sand samples were analyzed in certified laboratories at Qatar University.

Data pertaining to sand dunes in the Arabian deserts within the Mediterranean region has been acquired from the available literature. These data were mainly obtained from El-Oued region, northeast Sahara of Algeria and Erfoud area, southeastern of Morocco (Fig. 1) (Meftah and Hani, 2022; Meftah et al., 2021; Meftah and Mahboub, 2020; Adnani et al., 2016; Kabiri et al., 2003).

2.1.1 Analytical Methods

The physical and chemical characteristics of the sand dunes under study were assessed using several experimental techniques, including grain size analyses, X-ray fluorescence

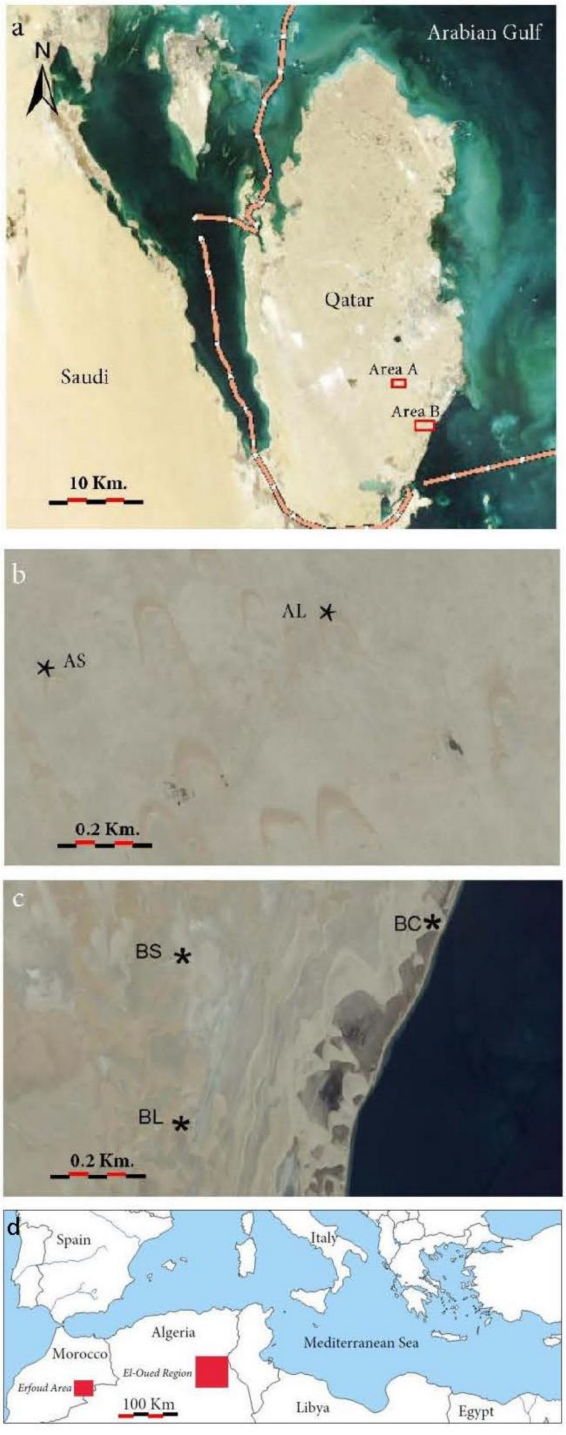

Figure 1. **(a)** Location map of the studied areas in Qatar (area A and area B); **(b)** Long (AL) and short (AS) dunes in area A; **(c)** Long (BL), short (BS) and costal (BC) dunes in area B; **(d)** Location map of El-Qued region, Algeria, and Erfoud area, Morocco. Satellite images courtesy of The Centre for GIS, Ministry of Municipality, Qatar.

Table 1. Distribution of the studied sand samples from Area A and Area B.

	Area A (Long dune sample #)	Area A (Short dune sample #)	Area B (Long dune sample #)	Area B (Short dune sample #)	Area B (Coast dune sample #)
Winward					
Crest	2	10	18	26	33
Middle	1	9	17	25	
Tail	6, 8	14, 16	22, 24	30, 32	
Leeward					
Crest	3	11	19	27	34
Middle	4	12	20	28	35
Tail	5, 7	13, 15	21, 23	29, 31	

(XRF), X-ray diffraction (XRD), scanning electron microscopy (SEM with energy dispersive spectrometry (EDS).

To determine the grain size distribution of the sand samples, thirty-five of them were analyzed using the Mastersizer 3000 analyzer manufactured by Malvern Panalytical. This compact optical system employs laser diffraction to measure particle size distribution ranging from 10 nm to 3500 µm, which is expressed in a set of size classes optimized to match the detector geometry and optical configuration, offering the best resolution. Prior to the analysis, the samples were dried in an oven at approximately 60° for 24 h and homogenized. A mass of 20 mg was selected from each sample.

To analyze the elemental composition of the sand samples, XRF analysis was performed using the Bruker S2 PUMA X-ray spectrometer. The Energy dispersive X-ray Fluorescence (EDXRF) spectroscopy technique was employed for qualitative and quantitative determination of the chemical elements. This device features a state-of-the-art HighSense detector and is powered by SPECTRA ELEMENTS software for elemental identification. The XRF analysis was able to detect element concentration ranging from parts per million (ppm) up to 100 % for all element masses starting from magnesium (Mg) up to uranium (U). Prior to the analysis, the samples were powdered and homogenized, and 10 gm from each sample was used.

To analyze the mineralogical composition of the sand samples, XRD analysis was carried out using the Empyrean XRD (PANalytical–EMPYREAN) device, which scanned the samples at a range between $5° \leq 2\theta \leq 90°$ with an increment of 0.01313°. This device employed detector anode materials, Cu-Ka, with radiation of 1.5425 Å. Highscore Plus version 4.5 software was used to interpret the data, which relied on Inorganic Crystal Structure Database (ICSD) and International Centre for Diffraction Data (ICDD) as a database library. Prior to the analysis, the sand samples were finely ground, homogenized, and the average bulk composition was determined.

The morphology and chemical composition of eleven representative sand samples were analyzed using the NOVA NANOSEM 450 instrument, which had a voltage capability ranging from 200 V to 30 kV and was equipped with an energy dispersive spectrometer (EDS) detector. Prior to the analysis, the samples were dried in an oven at approximately 60° for 24 h to remove humidity and then coated with a thin film of gold to enhance the interaction between the electron beam and the samples.

3 Results

3.1 Sand dunes of Southeastern Qatar

The sand samples obtained from both area A and area B exhibited a strikingly similar granulometry, chemical, and mineralogical composition. As a result, their characterizations were performed together. Any disparities that may exist in these properties will be highlighted and discussed in detail.

3.1.1 Grain size analysis

Grain size analysis was conducted on thirty-five samples. The resulting grain size data were presented in the form of histograms (Fig. 2). For each sample, five statistical parameters were calculated from the grain size distribution data, namely: the median (md), the graphic mean (Mz), the inclusive graphic standard deviation (σ_I), the inclusive graphic skewness (Sk_I), and the graphic kurtosis (K_G). These parameters were then classified according to the limits provided by Folk and Ward (1957). The grain size parameters obtained for the sand size fraction of the studied sediments are reported in Table 2.

Histograms

The dune sands in both areas are entirely composed of sand-sized grains. Histograms were constructed to display the mechanical composition of these grains. The histograms reveal

Table 2. Grain size parameters for the studied sand samples.

Area A, Long Dune (LS)								
Sample No.	1	2	3	4	5	6	7	8
K_G	0.95 Mesokurtic	0.94 Mesokurtic	0.94 Mesokurtic	0.95 Mesokurtic	1 mesokurtic	0.96 mesokurtic	0.94 mesokurtic	1 mesokurtic
Sk_I	0.01 Near symmetrical	0.05 Near symmetrical	0.03 Near symmetrical	0.01 Near symmetrical	0.13 fine skewed	0.16 fine skewed	0.04 near symmterical	0.13 fine skewed
σ_I	0.47 Well sorted	0.55 moderately well sorted	0.55 moderately well sorted	0.47 well sorted	0.62 moderately well sorted	0.79 moderately sorted	0.46 well sorted	0.66 moderately well sorted
Mz	1.81 Medimum grained	1.84 Medimum grained	1.82 Medimum grained	2.08 fine grained	1.33 medium grained	1.56 medium grained	1.17 medium grained	1.5 medium grained
Md	1.36	1.375	1.36	1.56	0.755	0.98	0.62	0.95
Area A, Short Dune (AS)								
Sample No.	9	10	11	12	13	14	15	16
K_G	0.94 mesokurtic	0.95 mesokurtic	0.94 mesokurtic	0.95 mesokurtic	0.93 mesokurtic	0.93 mesokurtic	0.94 mesokurtic	0.94 mesokurtic
Sk_I	0.02 near symmterical	0.01 near symmterical	0.02 near symmterical	0.01 near symmterical	0.03 near symmterical	0.02 near symmterical	0.04 near symmterical	0.01 near symmterical
σ_I	0.46 well sorted	0.48 well sorted	0.52 moderately well sorted	0.48 well sorted	0.46 well sorted	0.52 moderately well sorted	0.37 well sorted	0.55 moderately well sorted
Mz	1.89 medium grained	2.1 fine grained	2.12 fine grained	2.07 fine grained	1.86 medium grained	1.95 medium grained	1.35 medium grained	2 fine grained
Md	1.43	1.58	1.59	1.55	1.4	1.47	1.42	1.5
Area B, Long Dune (BL)								
Sample No.	17	18	19	20	21	22	23	24
K_G	0.98 mesokurtic	0.95 mesokurtic	0.96 mesokurtic	0.94 mesokurtic	0.95 mesokurtic	0.95 mesokurtic	0.97 mesokurtic	0.95 mesokurtic
Sk_I	−0.06 near symmterical	−0.02 near symmterical	−0.05 near symmterical	0.03 near symmterical	−0.03 near symmterical	0 near symmterical	−0.11 coarse skewed	−0.02 near symmterical
σ_I	0.6 moderately well sorted	0.57 moderately well sorted	0.62 moderately well sorted	0.55 moderately well sorted	0.56 moderately well sorted	0.52 moderately well sorted	0.73 moderately sorted	0.6 moderately well sorted
Mz	2.13 fine grained	2.16 fine grained	2.17 fine grained	1.61 medium grained	2.13 fine grained	2.2 fine grained	1.93 medium grained	1.95 medium grained
Md	1.6	1.64	1.65	1.14	1.6	1.655	1.45	1.46

Table 2. Continued.

Area B, Short Dune (BS)								
Sample No.	25	26	27	28	29	30	31	32
K_G	0.94 mesokurtic	0.95 mesokurtic	0.95 mesokurtic	0.95 mesokurtic	0.94 mesokurtic	0.98 mesokurtic	0.95 mesokurtic	0.97 mesokurtic
Sk_I	−0.02 near symmetrical	0.07 near symmterical	−0.01 near symmterical	0 near symmterical	0.01 near symmterical	−0.08 near symmterical	−0.02 near symmterical	−0.09 near symmterical
σ_I	0.61 moderately well sorted	0.6 moderately well sorted	0.58 moderately well sorted	0.56 moderately well sorted	0.63 moderately well sorted	0.69 moderately well sorted	0.57 moderately well sorted	0.72 moderately sorted
Mz	2.04 fine grained	1.67 medium grained	2.01 fine grained	1.88 medium grained	1.89 medium grained	2.08 fine grained	1.98 medium grained	1.91 medium grained
Md	1.54	1.19	1.51	1.41	1.41	1.58	1.49	1.44
Area B, Coastal Dune (BC)								
Sample No.	33	34	35					
K_G	0.9 mesokurtic	0.88 playtykurtic	0.9 mesokurtic					
Sk_I	0 near symmterical	0.03 near symmterical	0.03 near symmterical					
σ_I	0.83 moderately sorted	0.88 moderately sorted	0.83 moderately sorted					
Mz	1.82 medium grained	1.69 medium grained	1.75 medium grained					
Md	1.38	1.19	1.25					

unimodal distributions where the modal class falls into the fine and medium sand grades (Fig. 2).

Average size

The average size of the sand grains is determined using various statistical parameters. The simplest ones are the median and mean. For area A, the median diameter of the sand grains ranges from 0.62 to 1.59 ∅ (medium to coarse) with an average of 1.31 ∅ (medium). In contrast, for area B, the median diameter ranges from 1.14 to 1.66 ∅ (medium) with an average of 1.49 ∅ (medium). The graphic mean size (Mz) for area A ranges from 1.17 to 2.12 ∅ (fine to medium) with an average of 1.78 ∅ (medium). Around 31.25 % of the samples have fine grains, while 68.75 % have medium grains. In area B, the graphic mean size ranges from 1.61 to 2.20 ∅ (fine to medium) with an average of 1.98 ∅ (medium). Half of the samples have fine grains, while the other half have medium grains.

Standard deviation

In area A, the standard deviation values range from 0.37 to 0.79 ∅ (well-sorted to moderately sorted) with an average of 0.53 ∅ (moderately well-sorted). Around 6.25 % of the samples are moderately sorted, 43.75 % are moderately well-sorted, and 50 % are well-sorted. In contrast, for area B, the standard deviation values range from 0.52 to 0.73 ∅ (moderately well-sorted to moderately sorted) with an average of 0.61 ∅ (moderately well-sorted). Around 12.5 % of the samples are moderately sorted, while 87.50 % are moderately well-sorted.

Skewness

In area A, the skewness values range from 0.01 ∅ (nearly symmetric) to 0.16 ∅ (fine-skewed) with an average of 0.04 ∅ (nearly symmetric). About 81.25 % of the samples are nearly symmetric, while 18.75 % are fine-skewed. On the other hand, all the samples from area B are nearly symmetric,

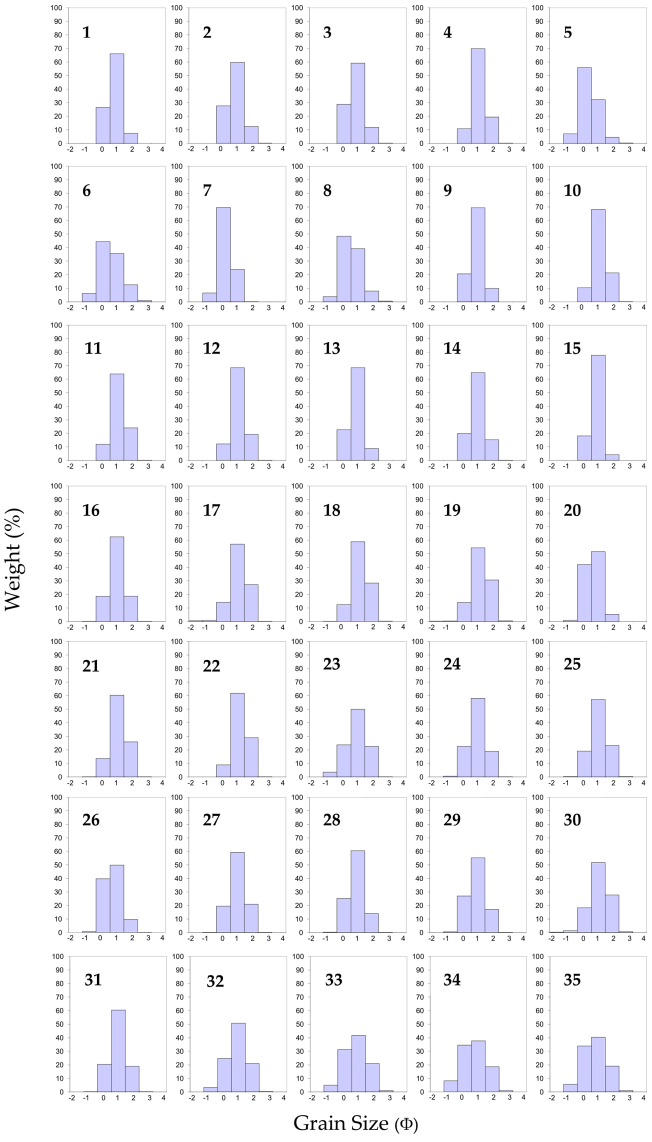

Figure 2. Histograms of grain size distribution for area A (1–16) and area B (17–35) sand samples showing a unimodal distribution.

with skewness values ranging from −0.10 to 0.07 ∅ (nearly symmetric) and an average of −0.025 ∅ (nearly symmetric).

Kurtosis

For area A, kurtosis ranges from 0.93 to 1.00 ∅ (mesokurtic) with an average of 0.95 ∅ (mesokurtic). Similarly, for area B, kurtosis values range from 0.94 to 0.98 ∅ (mesokurtic) with an average of 0.96 ∅ (mesokurtic).

3.1.2 Chemical Composition by X-Ray Fluorescence (XRF)

The XRF measurements reveal the chemical composition of the studied sand samples. The most abundant component in the samples is silicon oxide, which accounts for 58.1 % to 74.5 % of the total composition in area A and 63.7 % to 74.9 % in area B, with average values of 74.50 % and 74.90 %, respectively (Fig. 3).

Calcium oxide is the second most abundant component, making up 26.3 % of the total composition in area A and 15.0 % in area B, with average values of 18.3 % and 13.2 %, respectively.

Magnesium oxide is the third most abundant component, accounting for 17.80 % of the total composition in area A with an average of 7.90 %, and ranging from 1.50 % to 10.90 % in area B, with an average of 6.50 %.

Aluminum oxide is also present in significant amounts, ranging from 5.40 % to 8.90 % in area A and 6.40 % to 9.60 % in area B, with average values of 7.10 % and 6.50 %, respectively.

The sand samples from both areas contain low levels of other components, including Iron, Chlorine, Potassium, and Sulfur oxides, with maximum recorded values of 1.90 %, 1.30 %, 1.10 %, and 1.00 %, respectively. Traces of Ti, Sr, Cr, and Sc oxides are also detected, with the maximum recorded value of 0.6 % for Ti oxide in area A.

3.1.3 Mineralogical Composition by X-Ray Diffraction (XRD)

XRD investigation reveals that the sand samples are mainly composed of four minerals: Quartz, Protoenstatite, Calcite, and Feldspar (orthoclase and anorthoclase) (Figs. 4 and 5).

Quartz is the most abundant component, ranging from 49.00 % to 90.00 % in area A and 52.00 % to 88.00 % in area B, with average values of 70.63 % and 73.31 %, respectively (Figs. 4 and 5).

Protoenstatite makes up to 29.00 % of the total composition in area A and up to 32 % in area B, with average values of 20.50 % and 15.83 %, respectively (Figs. 4 and 5a).

Calcite ranges from 7.00 % to 26.00 % in area A and from 7.00 % to 18.00 % in area B, with average values of 17.50 % and 11.69 %, respectively (Figs. 4 and 5).

Both orthoclase and anorthoclase feldspars are present in the sand samples. Orthoclase makes up to 10.00 % of the total composition in area A with an average of 6.50 %, and in area B, it ranges from 3.00 % to 24.00 %, with an average of 11.50 % (Figs. 4 and 5c). Anorthoclase makes up to 20.00 % of the total composition in area A with an average of 8.64 %, and in area B, it ranges from 3.00 % to 35.00 %, with an average of 16.50 % (Figs. 4 and 5b, d).

Gypsum is only detected in the three sand samples collected from a sand dune near the coast (BC), with a maximum recorded value of 8.00 % (Figs. 4 and 5d).

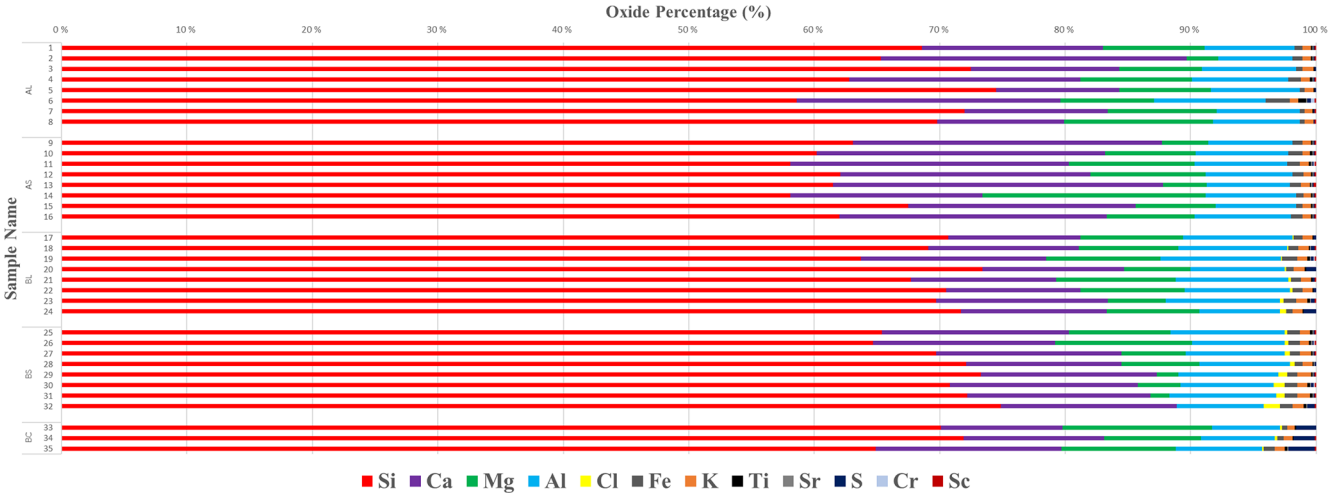

Figure 3. XRF analysis showing the elemental oxides forming the studied sand samples.

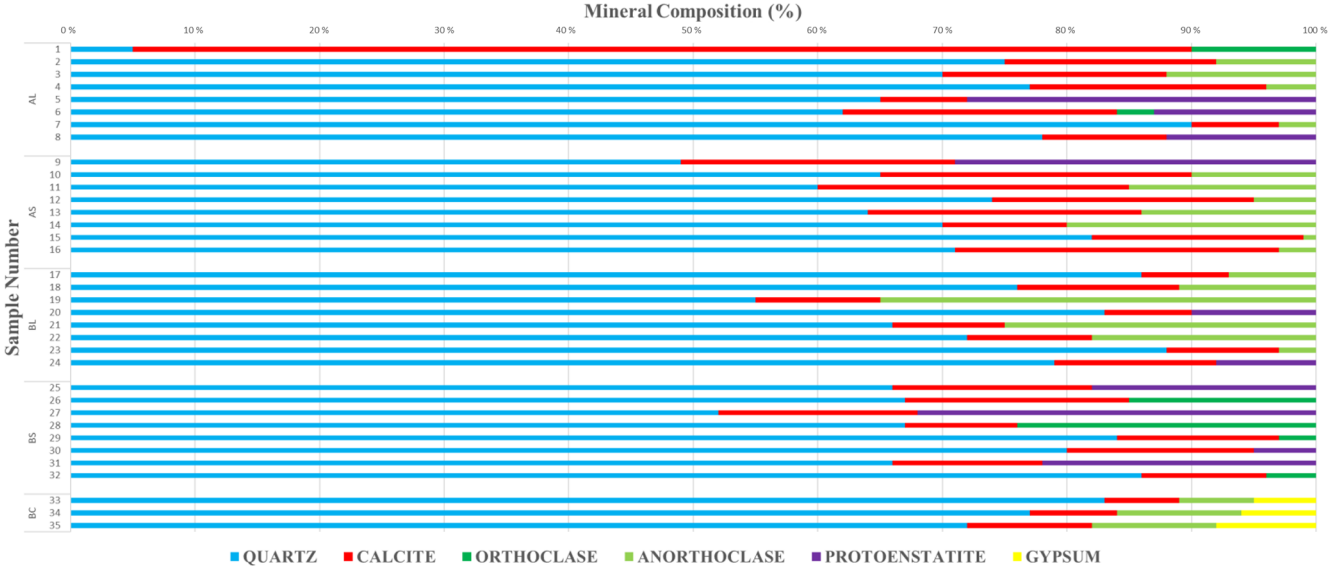

Figure 4. XRD analysis showing the major rock-forming minerals of the studied sand samples. Quartz is the dominating mineral followed by protoenstatite, calcite and feldspar minerals. Gypsum is present only in costal sand samples (33–35).

3.1.4 Morphology and Chemical Composition by Scanning Electron Microscopy with Energy Dispersive Spectrometry (SEM-EDS)

Enlarged images captured through SEM analysis revealed the morphology and texture of the sand samples under study (Figs. 6 and 7). When observed at lower magnifications, the constituent grains exhibited a range of shapes, ranging from angular to well-rounded with varying sphericity. Approximately 35 % of the grains were categorized as subrounded to rounded. The EDS profile analyses conducted on the sand samples provided insights into their elemental composition (Figs. 6 and 7). It was observed that the grains with rounded to well-rounded shapes had a higher concentration of calcium (up to 41.53 wt %, 21.57 at. %) and a lower concentration of silicon (1 wt %, 0.74 at. %) (Fig. 6c) compared with the angular to subangular grains, which were characterized by a higher silicon content (up to 45.36 wt %, 32.54 at. %) and a lower calcium content (2.81 wt %, 1.41 at. %) (Fig. 6d). Additionally, a few subrounded grains were found to have significant amounts of both calcium (28.53 wt %, 14.97 at. %) and silicon (12.95 wt %, 9.58 at. %) (Fig. 7c). The EDS analysis also revealed the presence of high sulfur content (up to 17.52 wt %, 11.36 at. %) in three samples collected from a dune located near the coast (Fig. 7d). The semi-quantitative chemical analysis conducted through EDS aligned well with the results obtained by means of XRD and XRF analyses.

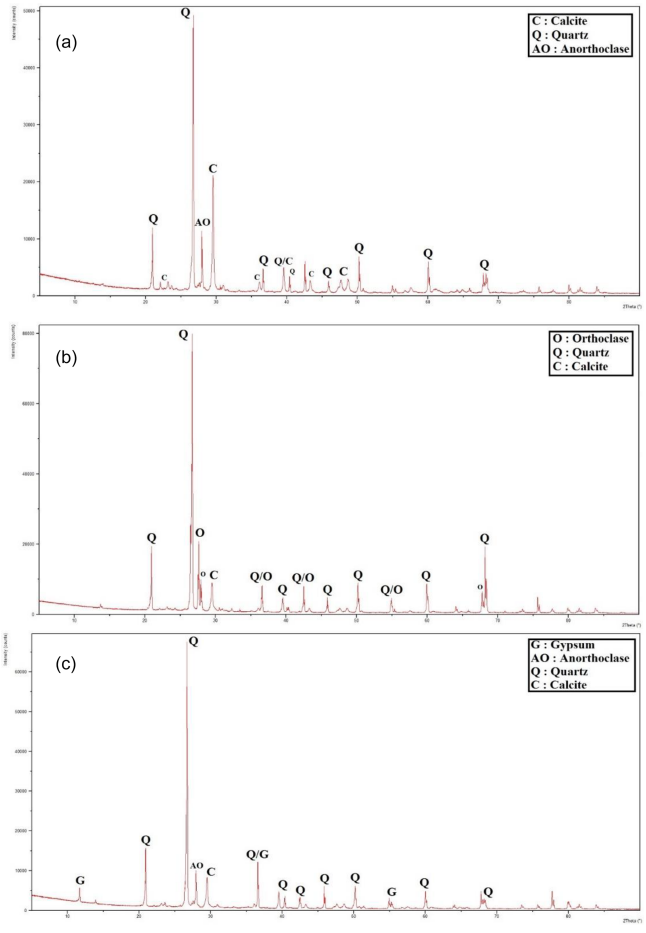

Figure 5. X-ray diffractograms showing quartz **(a–d)**; Protoenstatite **(a)**; calcite **(a–d)**; orthoclase **(c)**; anorthoclase and gypsum **(d)** mineral peaks.

3.2 Sand dunes of Arabian deserts, Mediterranean region

Information regarding sand dunes in the Arabian deserts within the Mediterranean region has been gathered from the existing literature. These data primarily originate from El-Oued region in the northeastern Sahara of Algeria and the Erfoud area in southeastern Morocco (Meftah and Hani, 2022; Meftah et al., 2021; Meftah and Mahboub, 2020; Adnani et al., 2016; Kabiri et al., 2003).

3.2.1 El-Oued region, Northeastern Sahara, Algeria

The sand dunes in El-Oued predominantly consist of approximately 97.63 % quartz (SiO_2) and 0.56 % calcite ($CaCO_3$), with notably low concentrations of other oxides such as Al_2O_3, Fe_2O_3, Na_2O, and MgO. Furthermore, the El-Oued sand has insignificant quantities of trace elements such as bromine (Br), germanium (Ge), bismuth (Bi), niobium (Nb), strontium (Sr), zinc (Zn), barium (Ba), and chlorine (Cl) (Meftah and Mahboub, 2020)

The sand grains exhibit a range of shapes, including rounded, elongated, angular, sub-angular, and irregular forms. The grains with irregular shapes are the most abundant. Additionally, the size of these sand grains varies within the range of 2.30 to 1.00 ∅ (fine to medium sand) (Meftah and Hani, 2022). Numerous mechanical and chemical effects are readily discernible on the surfaces of various sand grains. These eff ects include an abundance of small and medium-sized conchoidal fractures, V-shaped shock traces, both straight and curved grooves and scratches, dish-shaped concavities, crescentic percussion marks, bulbous edges, as well as solution pits, solution crevasses, and particles adhering to the surface (Meftah et al., 2021).

3.2.2 Erfoud area, Southeastern Morocco

The Yerdi sand dunes, situated in the southeastern region of Morocco near Erfoud, predominantly consist of a substantial quantity of quartz (SiO_2), accounting for up to 90 % of their composition. In contrast, the presence of calcite ($CaCO_3$) is relatively low, comprising no more than 8 % of the dune material. Additionally, there is a lesser presence of wustite (FeO) (Adnani et al., 2016).

The sand grains display a variety of shapes, which encompass rounded, angular, and sub-angular forms. The average size falls within the range of 2.19 to 2.59 ∅ categorizing the sand as fine sand. The symmetry, indicated by skewness, demonstrates that the distribution of sands is symmetric in comparison to its median, with values spanning from −0.001 to −0.01 ∅. The standard deviation, calculated from frequency curves, yields values between 0.40 and 0.55 ∅, indicating well-sorted sand. These findings are corroborated by the degree of grain concentration relative to the average, known as kurtosis, which ranges from 0.99 to 1.22 ∅. This indicates that the Yerdi sand ranges from being leptokurtic to mesokurtic in nature. The dunes in this area exhibit a rapid transition in color, shifting from a brownish-yellow hue to a reddish-yellow tone (Adnani et al., 2016).

4 Discussion

The studied Qatari sand samples from both areas are similar in nature. They fall within a small range of sand sizes, typically fine to medium, and display a unimodal distribution. It is possible that the limited range of sand sizes and unimodality are a result of the sediments present at the source area, as well as the NW Shamal wind's capacity to transport only a narrow range of sand sizes. They are moderately to well sorted and display a nearly symmetrical skewness with a mesokurtic shape. Despite being examined at various locations within the dune (tail, middle, or crest), under differing wind directions (windward or leeward), and with consideration to dune size (long or short), the granulometric properties of the sand samples do not demonstrate any significant

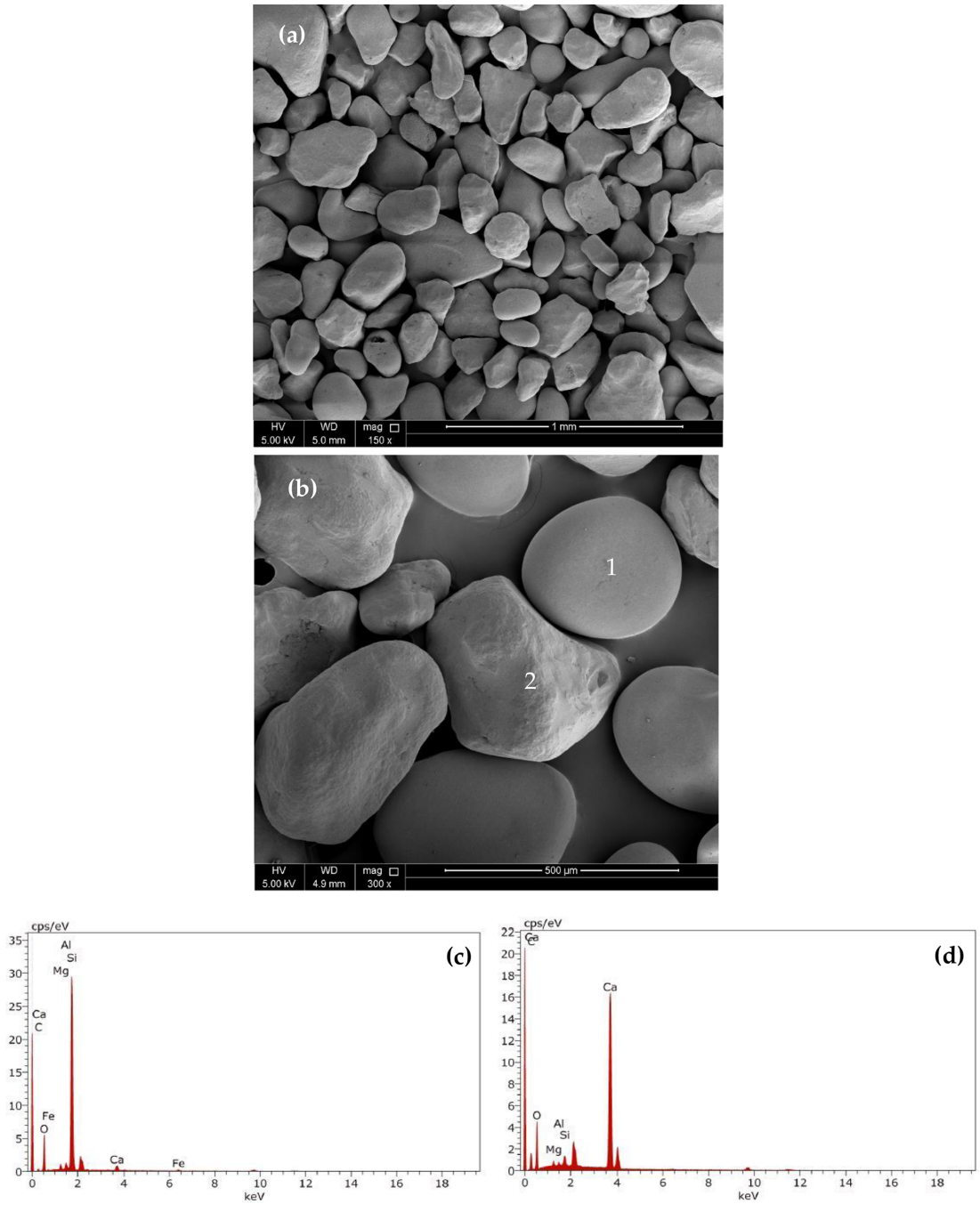

Figure 6. (a, b) SEM micrographs showing variable grain morphology and textures. Some grains have rounded outline and low relief; other grains show angular to subangular outline indicating nonuniform weathering. Elongated and disc shaped grains are also present. **(c)** EDS results of well rounded, low relief grain (1) having high amount of Ca and low amount of Si. **(d)** EDS results of subangular grain (2) having high amount of Si and low amount of Ca.

trends or noticeable changes. These characteristics may indicate that the sand dunes under study are inherited from the same provenance and may indicate aeolian origin.

The presence of diverse grain shapes, with irregular shapes being the most prevalent, within the sand dunes of the El-Oued region, along with the micro-textural characteristics marked by signs of collision and abrasion, may indicate that the El-Oued sand originated in an aeolian environment and subsequently underwent chemical alteration. On the other hand, the abundance of smooth, rounded quartz particles observed at Yerdi sand dunes may indicate a fluvial origin (Kabiri et al., 2003).

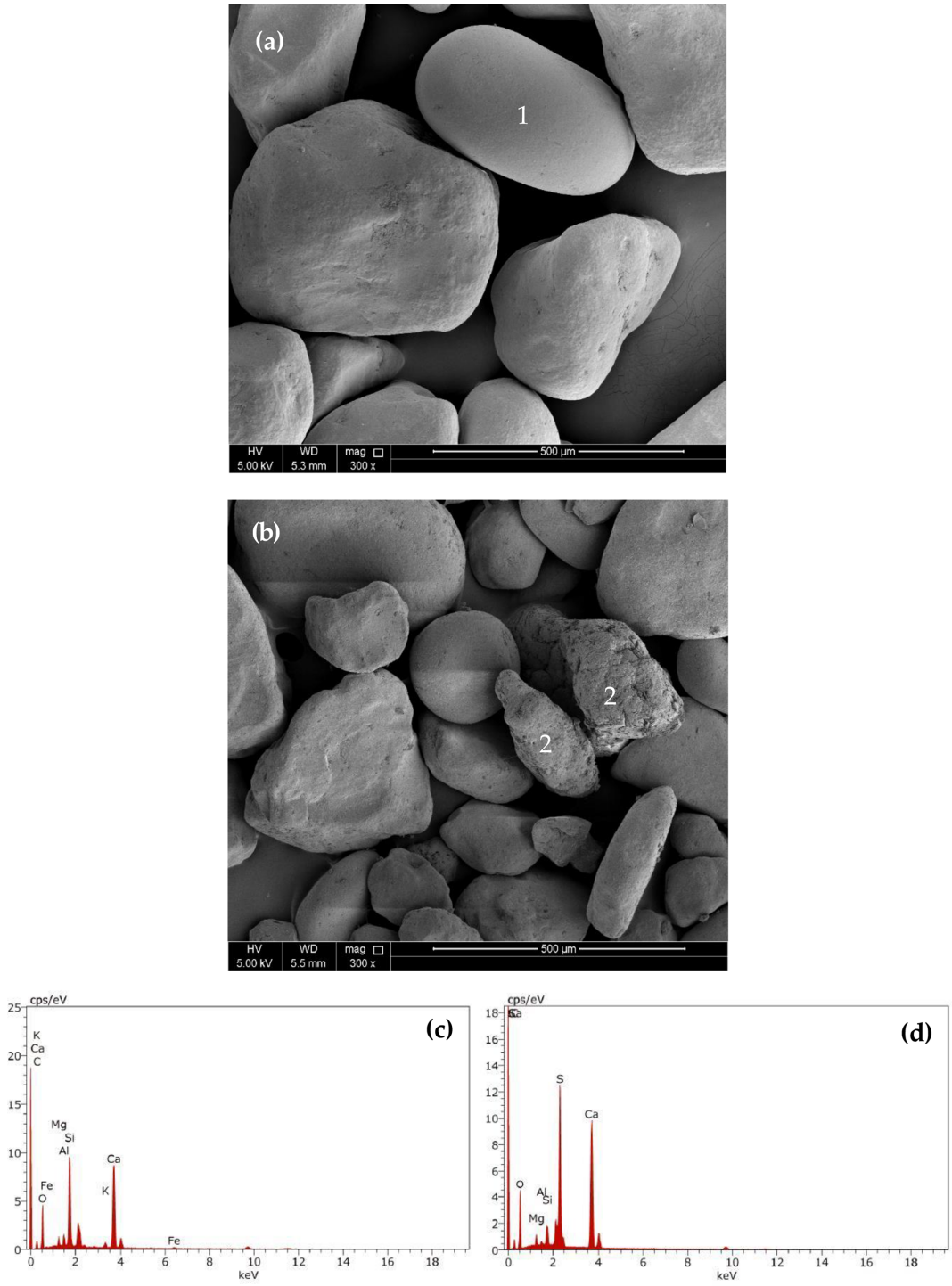

Figure 7. (a, b) SEM micrographs showing variable grain morphology and textures. **(c)** EDS results of a subrounded grain (1) showing considerable amounts of Ca and Si. **(d)** EDS results of a gypsum grain (2) showing high amount of S.

The studied Qatari sand dunes are mainly composed of silicates and carbonates. Clay minerals are relatively scarce. The silicates include quartz, protoenstatite, and feldspar, with quartz being the most common mineral. Protoenstatite is a variety of the silicate mineral enstatite. It is the stable form of magnesium silicate at very high temperatures (Cameron and Papike, 1981; Tribaudino et al., 2002). It was discovered in Oregon sunstones in 2017 by Xu et al. (2017), using high-resolution transmission electron microscopy (HRTEM) and X-ray energy-dispersive spectroscopy (EDS). The feldspar

content in the studied sand samples correlates well with that in coastal Jafurah and Liwa sand dunes as reported by Garzanti et al. (2013) in their study on the provenance and recycling of Arabian desert sand. During Pleistocene euostatic lowstand, the Arabian Gulf floor was exposed and loaded with materials supplied by tributaries draining Mesopotamian plain and the Zagros mountains (Garzanti et al., 2003). Later, these materials were blown inland by Shamal northerly winds.

The carbonates are mainly represented by calcite mineral, which is likely transported by Shamal winds from the local Tertiary sediments exposed on the surface of Qatar peninsula and the prevailing carbonate deposits in the region. The identified gypsum is believed to be the result of evaporation under arid conditions of highly saline seawater that percolated into sand dunes near the east coast of Qatar.

The presence of considerable proportions of unstable heavy minerals (epidote, garnet, pyroxene and amphibole), as reported by Nasir et al. (1999) in their study of the coastal sand dunes Southeastern Qatar, may suggest short transportation and low degree of weathering.

The compositional signature of the studied sand dunes is similar to that of the coastal Jafurah and Liwa sand dunes in being carbonaticlastic rich in feldspar, indicating that these coastal sand dunes are mostly driven from similar sources. On the other hand, it differs from the inland sand dunes in the neighboring regions characterized by high quartz content, few feldspar grains, and rare carbonate minerals as reported by Garzanti et al. (2003).

The grains with angular and subangular shapes primarily consist of silicates, specifically quartz, while the rounded, subrounded, and disc-shaped grains are primarily composed of carbonates, specifically calcite. The angularity observed in the quartz grains can be attributed to their high resistance against the abrasive impact of the NW Shamal wind during transportation. In contrast, the carbonate grains are less resistant to the abrasive effects of the NW Shamal wind, resulting in their rounded shape. It is worth noting that the process of abrasion does not cause any systematic change in the roundness and sphericity of carbonate grains as they are transported downwind.

The composition of sand dunes in both El-Oued and Yerdi primarily consists of silicates and carbonates, which is akin to the composition found in Qatari sand dunes. However, there is a notable distinction in the quantities of quartz and carbonates present. Specifically, there is a significantly higher proportion of quartz and a reduced amount of carbonates in the Mediterranean sand dunes when compared to those in Southeastern Qatar. This discrepancy underscores the exceptional purity of the quartz sand found in these Mediterranean sand dunes in contrast to the sand dunes in Southeastern Qatar.

The impurity observed in the sand dunes of Qatar's study area relative to the Mediterranean sand dunes can be attributed to the prevalence of carbonate minerals, which are sourced from abundant carbonate-rich rocks in the Arabian Peninsula.

5 Conclusions

The physiochemical properties of the studied Qatari sand dunes indicate that they are driven from the same provenance and may have aeolian origin. Likewise, the characteristics of El-Oued sand point to an aeolian origin. Conversely, Yerdi sand dunes are indicative of a possible fluvial (river-driven) origin. The composition of the studied Qatari sand dunes reveals a mixture of siliceous and calcareous materials. They contain abundant quartz, protoenststite, calcite, and feldspar minerals, while clay minerals are relatively scarce. Conversely, the sand dunes in the Mediterranean region exhibit a comparable composition but with a higher concentration of siliceous materials and a lower proportion of calcareous components. They contain abundant quartz and low calcite. The mineralogical composition of the studied Qatari sand dunes suggests substantial contributions from the Mesopotamian plain, Zagros Mountains, and the calcareous coast of the Arabian Gulf. These sources influenced the composition of the sand dunes significantly.

The chemical composition of the Qatari sand samples shows high concentrations of silicon oxide, and significant concentrations of calcium, magnesium, and aluminum oxides, with small amounts of Iron, Chlorine, Potassium, and Sulfur oxides, and insignificant amounts of other trace elements such as Ti, Sr, Cr, and Sc oxides. In contrast, the sand dunes in the Mediterranean region exhibit a similar composition, but with higher concentrations of silicon oxide and reduced levels of calcium.

Considering the silicon content, it's worth noting that the Qatari sand dunes, overall, exhibit a lower degree of purity in comparison to the Mediterranean dunes. Consequently, careful processing is imperative before utilizing these sands in industrial applications. Additionally, the presence of carbonates and gypsum in the Qatari sands poses potential challenges for the quality of concrete and mortars. As a result, it is essential to employ techniques that can enhance the sand's quality before incorporating it into construction applications in Qatar, whether it be for concrete or mortar production.

Data availability. All data for this study are presented in the paper: Tables 1–2, Figs. 2–7, and Sect. 3.

Author contributions. Conceptualization, HAA; sample collection and methodology, HAA and WSM; validation, HAA and WSM; formal analysis, HAA and WSM; writing-original draft preparation, HAA and WSM; writing-review and editing, WSM; visualization, HAA and WSM; supervision, HAA and WSM; project administration, WSM; funding acquisition, HAA. The authors have read and agreed to the published version of the manuscript.

Competing interests. The contact author has declared that neither of the authors has any competing interests.

Disclaimer. Publisher's note: Copernicus Publications remains neutral with regard to jurisdictional claims made in the text, published maps, institutional affiliations, or any other geographical representation in this paper. While Copernicus Publications makes every effort to include appropriate place names, the final responsibility lies with the authors.

Special issue statement. This article is part of the special issue "New advances on the geology of the central–western Mediterranean area (EGU 2023 SSP1.7 session)". It is a result of the EGU General Assembly 2023, Vienna, Austria, 23–28 April 2023.

Acknowledgements. The SEM-EDS analysis was performed at Qatar University's Central Laboratory Unit (CLU). We sincerely appreciate their unwavering support and professionalism. Our gratitude goes to the Center for Advanced Materials (CAM) at Qatar University for conducting the XRF and XRD analyses. Lastly, we extend our heartfelt thanks to the Environmental Science Center (ESC) at Qatar University for carrying out the textural analyses.

Review statement. This paper was edited by Roberta Somma and reviewed by Roberta Somma and one anonymous referee.

References

Adnani, M., Azzaoui, M. A., Elbelrhiti, H., Ahmamou, M., Masmoudi, L., and Chiban, M.: Yerdi sand dunes (Erfoud area, southeastern of Morocco): color, composition, sand's provenance, and transport pathways, Arab. J. Geosci., 9, 366, https://doi.org/10.1007/s12517-016-2394-x, 2016.

Al-Ansary, M., Pöppelreiter, M. C., Al-Jabry, A., and Iyengar, S. R.: Geological and physiochemical characterisation of construction sands in Qatar, Int. J. Sustain. Built Environ., 1, 64–84, https://doi.org/10.1016/j.ijsbe.2012.07.001, 2012.

Al-Saad, H.: Lithostratigraphy of the Middle Eocene Dammam Formation in Qatar, Arabian Gulf: effects of sea-level fluctuations along a tidal environment, J. Asian Earth Sci., 25, 781–789, https://doi.org/10.1016/j.jseaes.2004.07.009, 2005.

Al-Saad, H. and Ibrahim, M. I.: Stratigraphy, micropaleontology, and paleoecology of the Miocene Dam Formation, Qatar, GeoArabia, 7, 9–28, https://doi.org/10.2113/geoarabia070109, 2002.

Alsharhan, A. S. and Nairn, A. E. M.: Stratigraphy and sedimentology of the Permian in the Arabian basin and adjacent areas: a critical review, The Permian of Northern Pangea, 2, 187–214, https://doi.org/10.1007/978-3-642-78590-0, 1995.

Al-Yousef, M.: Mineralogy, geochemistry and origin of Quaternary sabkhas in the Qatar Peninsula, Arabian Gulf, Ph.D. Thesis, University of Southampton, Southampton, UK, ISNI: 0000 0001 3409 455X, 2003.

Ashour, M. M.: Textural properties of Qatar dune-sands, J. Arid Environ., 8, 1–14, https://doi.org/10.1016/S0140-1963(18)31333-8, 1985.

Boukhary, M.: Paleontological studies on the Eocene succession in western Qatar, Arabian Gulf, Rev. Paleobiologie, 4, 183–202, 1985.

Cameron, M. and Papike, J. J.: Structural and chemical variations in pyroxenes, Am. Mineral., 66, 1–50, 1981.

Embabi, N. S. and Ashour, M. M.: Barchan dunes in Qatar, J. Arid Environ., 25, 49–69, https://doi.org/10.1006/jare.1993.1042, 1993.

Engel, M., Boesl, F., and Brückner, H.: Migration of barchan dunes in Qatar–controls of the Shamal, teleconnections, sea-level changes and human impact, Geosciences, 8, 240, https://doi.org/10.3390/geosciences8070240, 2018.

Folk, R. L. and Ward, W. C.: Brazos River bar (Texas): a study in the significance of grain size parameters, J. Sediment. Res., 27, 3–26, https://doi.org/10.1306/74D70646-2B21-11D7-8648000102C1865D, 1957.

Garzanti, E., Ando, S., Vezzoli, G., and Dell'era, D.: From rifted margins to foreland basins: investigating provenance and sediment dispersal across desert Arabia (Oman, UAE), J. Sediment. Res., 73, 572–588, https://doi.org/10.1306/101702730572, 2003.

Garzanti, E., Vermeesch, P., Andò, S., Vezzoli, G., Valagussa, M., Allen, K., Kadi, K. A., and Al-Juboury, A. I.: Provenance and recycling of Arabian desert sand, Earth-Sci. Rev., 120, 1–19, https://doi.org/10.1016/j.earscirev.2013.01.005, 2013.

Kabiri, L., Boudad, L., Krimou, A., Khardi, A., and Elmrani, L.: Etude préliminaire de la dynamique des dunes continentales dans le Sud Est marocain, Sci et Changement Planétaire, 14, 149–156, https://api.semanticscholar.org/CorpusID:128633737, 2003.

Meftah, N. and Hani, A.: Characterization of Algerian dune sand as a source to metallurgical-grade silicon production, Mater. Today, 51, 2105–2108, https://doi.org/10.1016/j.matpr.2021.12.366, 2022.

Meftah, N. and Mahboub, M. S.: Spectroscopic characterizations of sand dunes minerals of El-Oued (Northeast Algerian Sahara) by FTIR, XRF and XRD analyses, Silicon, 12, 147–153, https://doi.org/10.1007/s12633-019-00109-5, 2020.

Meftah, N., Hani, A., Merdas, A., Sadik, C., and Sdiri, A.: A holistic approach towards characterizing the El-Oued siliceous sand (eastern Algeria) for potential industrial applications, Arab. J. Geosci., 14, 1–14, https://doi.org/10.1007/s12517-021-08591-1, 2021.

Michel, S., Avouac, J. P., Ayoub, F., Ewing, R. C., Vriend, N., and Heggy, E.: Comparing dune migration measured from remote sensing with sand flux prediction based on weather data and model, a test case in Qatar, Earth Planet. Sc. Lett., 497, 12–21, https://doi.org/10.1016/j.epsl.2018.05.037, 2018.

Nasir, S. J., El-Kassas, I. A., and Sadiq, A. A. M.: Mineralogy and genesis of heavy minerals in coastal dune sands, South Eastern Qatar, Qatar University Sci. J., 19, 184–201, http://hdl.handle.net/10576/9882, 1999.

Powers, R. W., Ramirez, L. F., Redmond, C. D., and Elberg, E. L.: Geology of the Arabian Peninsula, Sedimentary Geology of Saudi Arabia, USGS, Professional Paper 560-D, 147, https://doi.org/10.3133/pp560D, 1966.

Rao, P. G., Al-Sulaiti, M., and Al-Mulla, A. H.: Winter Shamals in Qatar, Arabian Gulf, Weather, 56, 444–451, https://doi.org/10.1002/j.1477-8696.2001.tb06528.x, 2001.

Sadiq, A. and Howari, F.: Remote sensing and spectral characteristics of desert sand from Qatar Peninsula, Arabian/Persian Gulf, Remote Sens., 1, 915–933, https://doi.org/10.3390/rs1040915, 2009.

Sankaran, R., Zouari, N., Sadooni, F. N., Al Disi, Z. A., Al-Jabri, A., and Al-Kuwari, H. A.: Mapping of aeolian deposits of an industrial site in the arid region using the TIR bands of ASTER and study of physicochemical characters and stabilization of sand erosion, Geomat. Nat. Haz. Risk, 13, 2535–2559, https://doi.org/10.1080/19475705.2022.2122873, 2022.

Scheibert, C., Stietiya, M., Sommer, J., Schramm, H., and Memah, M.: The Atlas of soils for the State of Qatar, soil classification and land use specification project for the State of Qatar, Ministry of Municipal Affairs and Agriculture, General Directorate of Agricultural Research and Development, Department of Agricultural and Water Research, Ministry of Municipal Affairs and Agriculture, Doha, 2005.

Tribaudino, M., Nestola, F., Cámara, F., and Domeneghetti, M. C.: The high-temperature P 21/c-C 2/c phase transition in Fe-free pyroxene (Ca0. 15Mg1. 85Si2O6): Structural and thermodynamic behavior, Am. Mineral., 87, 648–657, 2002.

Xu, H., Hill, T. R., Konishi, H., and Farfan, G.: Protoenstatite: A new mineral in Oregon sunstones with "watermelon" colors, Am. Mineral., 102, 2146–2149, 2017.